RSC Advances

ROYAL SOCIETY OF CHEMISTRY

www.rsc.org/advances

RSC Advances

RSCPublishing

ARTICLE

Nanostructured Superhydrophobic Silk Fabric Fabricated Using the Ion Beam Method

Cite this: DOI: 10.1039/x0xx00000x

Ji-Hyun Oh [ab], Tae-Jun Ko [b], Myoung-Woon Moon [b*], and Chung Hee Park [a**]

Received ooth January 2012,
Accepted ooth January 2012

DOI: 10.1039/x0xx00000x

www.rsc.org/

Superhydrophobic silk fabric surfaces with high-aspect-ratio nanostructures were fabricated using ion beam treatment. The ion beam irradiated silk fabrics were characterized in terms of wettability, as well as other physical properties unique to silk. The nanostructures were produced in various configurations, ranging from columnar to hairy shapes, on the silk fibers through anisotropic etching with oxygen ion beam treatment. With subsequent hydrophobic coating on the nanostructured, superhydrophobic silk fiber surfaces were achieved with the increase of the static contact angle from 0° for the pristine hydrophilic silk fabric to 170° for the superhydrophobic silk fabric and with the decrease of shedding angle by less than 5°, which is sufficient to cause a water droplet to roll-off from the silk fabric surface. Because the ion beam-treated side of silk fabric become superhydrophobic, while the opposite side, or body contacting side, remains pristine or superhydrophilic, an extremely asymmetric wettability can be achieved in the silk fabric, which improves its breathability by improving moisture transmittance through a fabric from the body to the outer surface. The luster and color of silk fabric before and after ion beam irradiation were found to exhibit no significant degradation. Breaking load of the silk fabric after the ion beam treatment was assessed to be mechanically durable in comparison to that of the pristine fabric. Therefore, after introducing the superhydrophobic property via the ion beam treatment, the silk fabric maintained its primary advantages; as a result, the range of its applications can expand into breathable self-cleaning clothing textiles, such as neckties, blouses and dresses.

1. Introduction

Silk is a natural protein fabric having prominent characteristics of luster, handle, toughness and breathability, which broaden its application for various fields, such as textiles, cosmetics, membrane materials, and medical biomaterials.[1, 2] However, being composed of degradable proteins, wearable textiles made of silk have disadvantages, such as staining and low-water resistance. In particular, the mechanical properties of silk fibers submerged in water decrease because water weakens hydrogen bonds and reduces the van der Waals between chain segments in the amorphous phase of silk.[3] Furthermore, surface cleaning should be performed with dry-cleaning solvents, such as perchloroethylene, which has environmental disadvantages because of its toxicity.[4] Accordingly, it is important for silk fabric to overcome staining and water-related issues to enable its use in applications for which washing with water is required.

For developing the hydrophobicity of silk, water repellent finishing has been adopted, which can be implemented using various methods. One of those methods is a padding or impregnation process, which is a typical means to improve textile hydrophobicity. This method, however, has several problems, such as the decrease of vapor permeability, which cause wearing discomfort. Coating finishing is also used to improve the property of hydrophobicity on silk, but it exhibits low durability, making this method inappropriate for practical use. Another method, chemical grafting, is not always environmentally friendly and may change in the mechanical properties of silk.[5] Additionally, due to the reduction of unique advantages of silk, such as luster, textile, vapor permeability, and so on, a chemical-based finishing process to convert silk into usable materials may be inapplicable to luxurious silk.

Due to the mechanical weakness of silk in wet condition, silk needs to have water resistance, superhydrophobicity. The methods to induce superhydrophobicity on the surfaces can be divided into three categories[6]: top-down approaches (nano-imprinting[7], template-based technique[8] and e-beam[9, 10] or plasma treatment[11]), bottom-up approaches (layer-by-layer (LBL) deposition[12], hydrogen bonding[13] and colloidal assemblies[14]) and a combination of both top-down and bottom-up approaches (casting of polymer solution and phase separation[15] and electro-spinning with chemical vapor

deposition[16]). Among those methods, developed the plasma or ion beam treatment has been widely used to produce a hydrophobic surface on polymers and textile materials, resulting in a value of a static contact angle of over 150° and a contact angle hysteresis of less than 10°. This process is known to be a rapid and environmentally friendly method that does not interfere with the bulk properties and can treat one side of a textile.[17, 18] For example, Li et al.[19] developed a hydrophobic habutai silk exhibiting the static contact angle of 123° and a wet-out time of over 60 min using a hexafluoropropene (C_3F_3) plasma treatment. Several works also suggested that the plasma treatment would improve hydrophobicity, as well as reducing the contact angle hysteresis to a value as low as 5° on various textile materials, such as silk or polypropylene.[20-22] However, no reports have yet provided superhydrophobic silk fabrics.

It is known that moisture transmittance through a fabric is a main factor to enable comfort in the clothing climate, which could be controlled by asymmetric wettability, i.e., having one side be a hydrophobic fabric while having the other or opposite side be hydrophilic. A fabric with the asymmetric wettability exhibits unidirectional water flow, i.e., water, oil, bacteria and germs are repelled on the one surface with self-cleaning property, while water vapor is absorbed on the other side, resulting in a comfortable, breathable and low-skin-irritating fabric. Thus, the surface with asymmetric wettability is an interesting and important component apparel applications.[23] The development of the asymmetric or unidirectional water permeability surface has progressed further in recent years. Kong et al.[24] reported that after irradiating solar or UV light onto a piece of cotton coated with TiO_2, the surface of the cotton piece exhibited superhydrophobicity because of a photo-induced phenomenon of TiO_2, while the opposite side of the cotton preserved its hydrophobicity, with 140° of static contact angle. Lim et al.[25] demonstrated extremely the asymmetric wettability on a fabric formed by electro-spinning of polyacrylonitrile and its hydrolysis. For the fabric exhibiting the asymmetric wettability, water repellency or easy cleaning is exhibited on its outer surface, while the unique properties of clothing comfort are maintained on its inner surface. In addition to the asymmetric property, the superhydrophobic silk fabrics could be used for a broader range of applications, e.g., use in rainy weather or being easily managed by reducing the number of washings required.

In this study, we introduced a novel method to fabricate the nanostructured superhydrophobic silk fabrics based on the ion beam treatment of oxygen etching and subsequent hydrophobic deposition. The nanostructured silk fabrics were characterized by measuring the static contact angle, the shedding angle, the water repellency for various liquids that could be stained on the silk fabrics in daily life (see Fig. 1a), and the unidirectional water absorption. Chemical analysis was performed, focusing on the change in chemical composition of silk before and after the ion beam treatment. Furthermore, we examined the unique silk properties by measuring the luster and color values of the nanostructured silk fabric. The breaking load of silk fabric was carefully measured before and after immersing in water onto the surfaces of both pristine and superhydrophobic silk fabrics.

2. Experimental

Fabrication of superhydrophobic silk

Silk fabric (#615 ISO Silk Adjacent Fabric [ISO 105/F06], Test Fabrics Co. USA) was used for this study. The silk fabric was Plain Habutai silk fabric consisting of three doubling yarns (warp count-30.2-3d, weft count-20.2-3d), fabric count of 53 × 36/cm and weight of 60.277 g/m^2. To prepare the superhydrophobic surface, the ion beam method was adopted involving the initial ion beam etching step to form nanostructures on the silk fabrics and the subsequent ion beam deposition step to render the nanostructured surfaces superhydrophobic. O_2 gas was first introduced into the anode of the linear ion source to produce oxygen ions. The distance between ion source and substrate was kept at 150 mm. The gas flow rate was set at 3.5 sccm and the total gas pressure was stable at 35-50 mTorr. The ion beam power and substrate bias voltage were 100 W and -400 V, respectively. The duration of the oxygen ion beam irradiation was varied from 0 to 10 min, resulting in various nanopatterns, ranging from dot to hair-like structures. Next, mixture gases of C_2H_2 and CF_4 with a ratio of 4 to 16 sccm were used for the ion beam deposition of a fluorinated diamond-like carbon (F-DLC) film onto the nanostructured silk fabrics for 30 sec with the deposition rate of 44 nm/min to deposit a low-surface-energy coating. The surface energy of the F-DLC coatings showed 31.57 mN/m, which resulted in the previously measured 81.3 ± 0.3° of the static contact angle on a flat stainless steel disc surface.[26] The working pressure was stabilized at 150 mTorr. The ion discharge power for ion beam and bias voltage was applied under the same conditions as those of the oxygen ion beam irradiation.

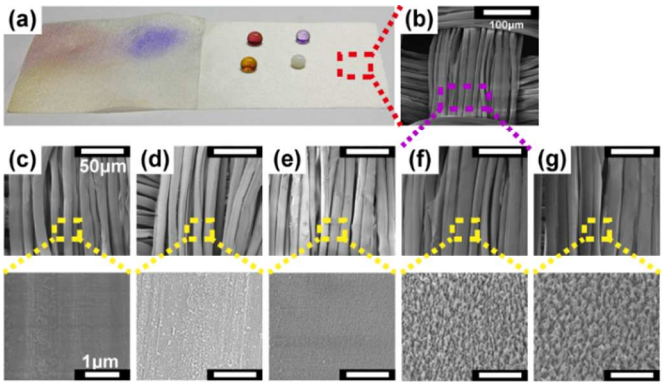

Fig. 1 (a) a photographic image of grape juice (purple), water droplet (dyed by violet), coffee (brown) and milk (white) on the silk surfaces before (left) and after (right) superhydrophobic ion beam treatment. Here, the superhydrophobic silk fabric surface was etched by the oxygen ion beam for 5 min and subsequently coated with the F-DLC coating for 30 sec on the right half fabric., (b) an SEM image of the superhydrophobic silk fabric etched for 5 min (magnified to 500 ×). (c-g) SEM images of the silk fibers irradiated by the oxygen ion beam irradiation for different exposure durations: (c) pristine (d) 1 min, (e) 2 min, (f) 5 min and (g) 10 min (magnified to 1,000 × for the upper images and 40,000 × for the lower images).

SEM, XPS analysis and water behavior measurement

The nanostructures on silk fabric were imaged using a scanning electron microscope (SEM, Nova NanoSEM 200, FEI, USA). Before the SEM observation, a 10-nm thick Pt film was coated onto the substrates to avoid electron charging on the silk fabric surface. The electron accelerating voltage of the SEM was 10 kV. The aspect ratio, defined as the ratio of height over width, of nanostructures was estimated on the silk fiber by direct measurement in SEM images magnified at 40,000 × with

a tilting angle of 30°. The width and height was measured with Image J program. The chemical composition of pristine and superhydrophobic silk fabric was analyzed using X-ray photoelectron spectroscopy (XPS, Axis-HSI instrument, Kratos Inc., USA). The hemispherical analyzer equipment was equipped with an Mg/Al dual anode x-ray source used in Mg K_{α} mode with a pass energy of 20 eV and an energy resolution of 0.1eV. The photoelectron spectrum was recorded with the x-ray source operating at 150 W (10 mA × 15 kV).

The wetting behavior of each sample was evaluated by performing the static contact angle, the shedding angle and the water droplet bouncing measurements. To determine the static contact angle of deionized (DI) water, 3.40 ± 0.3 μl in volume of DI water was deposited onto the silk surface, and the static contact angle was measured using a contact angle goniometer (Theta Lite, Attension, Finland). The shedding angle was measured using the same equipment used for the static contact angle measurement. We used the shedding angle methodology developed by Jan Zimmermann.[27] The shedding angle was determined by the measured angle at which a water droplet with 12.5 ± 0.1 μl in volume rolled off over 2 cm. The distance between a syringe tip to the sample surface was fixed at 10 mm.

The rain resistance of each silk fabric sample was tested by a water droplet impacting experiment (droplet bouncing movie) that simulates a raindrop from sky. By releasing the water droplet onto the surface from a syringe tip at the height of 70 mm from the fabric surface, the bouncing or penetration through the silk fabric surface was recorded. The bouncing movie on both the pristine and superhydrophobic silk fabric was recorded using a high-speed motion camera (Motion Pro® HS-4, Redlake Imaging, USA) with a frame rate of 500 fps (pristine silk) and 1000 fps (superhydrophobic silk).

Analysis of the luster and color change

The luster property of silk fabrics before and after ion beam irradiation was determined using a goniophotometer (GP-200, Murakami Color Research Laboratory, Japan). One fixed light source of spot size of 5 mm illuminated one point of the substrate at 30°. The incident light was detected by a detector arranged at an angle ranging from -75° to +90° at every 0.1°. Because some research studies reported that plasma treatment on a surface affects the surface yellowing[28], we also assessed the color value, which was measured according to the values of L* (whiteness vs. darkness), a* (red vs. green) and b* (yellow vs. blue) using a spectrophotometer (CM-2600d , Konica Minolta, Japan).[29]

Measurement of the mechanical property

The mechanical property of the silk fabric before and after ion beam irradiation was measured to monitor the breaking load with and without pouring distilled water onto each of the silk surfaces. The load-extension curve was obtained by using a Universal Testing Machine (Instron-5543, Instron, USA). The experiment was performed according to the ASTM D 5035 strip method. The size of each of the substrates was prepared with a width of 35 mm and a length of 160 mm. On a square glass dish (185 mm × 185 mm), each substrate was taped around the four edges at intervals of 5 mm. Next, 150 ml of DI water was poured over the glass dish until the surface of substrate was completely immersed, and the immersion was maintained for 30 sec. The mechanical test for the breaking load was performed after discarding water and successively cutting the four edges attached by a tape. A clamp interval was configured with 76 mm. 10 N of load and 100 mm/min of tension speed were applied until the sample was broken. Three samples with and without the ion beam etching and deposition were averaged under the same loading and speed conditions.

3. Results and discussion

The wettability for various liquid droplets was demonstrated on the silk fabric, for which half of the region was changed to the superhydrophobic surface, while the other half remained as the water-absorbable and hydrophilic surface. Several droplets of liquids of grape juice (purple), water droplet (dyed by violet), coffee (brown) and milk (white) were gently placed onto the silk fabric. As shown in Fig. 1a, after the placement of each of the liquid droplets, the pristine silk fabric immediately absorbed all of the liquids, became stained with its dye colors and even became bent as a result of the swelling due to its hydrophilic nature. In contrast, each of the liquid droplets retained a spherical shape when placed onto the superhydrophobic silk fabric, which can repel the droplets and even roll liquid off easily.

Nanostructured Silk

The surfaces of the silk fibers before and after the oxygen ion beam irradiation that varied from 0 to 10 min were characterized, as shown in Fig. 1b-g. With an increase of the oxygen ion beam irradiation on the silk fibers, the surface patterns were observed to evolve to produce various configurations, such as dots, pillars and hairs. As shown in the geometries of the nanostructures in the insert images of Fig. 1b-g, an aspect ratio (defined as the proportional relationship between a width and height) of the nanostructures linearly increased with the ion beam exposure duration. At the initial stage of 1 min and 2 min of the oxygen ion beam irradiation, the surface structures on the silk fibers appeared as the ripple and embossed structures, of which the aspect ratio is a value of approximately 1. After 5 min of the oxygen ion beam irradiation, the aspect ratio increased distinctively up to approximately 10. It was reported that the nanostructures on polymeric surfaces were formed by a selective etching mechanism with co-deposition of hard inhibitors, which originated from metallic reactor walls or chamber.[30] The metallic elements were co-deposited onto the target surface during the ion beam irradiation of the sample surface, where the regions covered by the hard metallic elements. The etching inhibitors are hardly etched, while the other regions with no metallic elements are rapidly etched due to the high rate of reaction between the oxygen ion beam and carbon-based polymeric surfaces. The reactive oxygen ions break the polymer C–C backbone and produce volatile species, such as CO or CO_2. Consequently, with the increase of the ion beam irradiation duration, the aspect ratio increased and the surface became roughened and textured, such as those shown in Fig. 1b-g.[30]

XPS result analysis before and after ion beam deposition

To explore the surface property of the silk fabrics before and after the oxygen ion beam irradiation and hydrophobic deposition, the chemical analysis of the pristine and superhydrophobic silk fabrics was performed, as shown in Fig. 2. A survey spectra for the pristine silk fabric revealed the spectral peaks for C1s, O1s and N1s, which is similar to

reported peaks for silk fabrics.[17] However, an F1s spectral peak was only detected in the superhydrophobic silk fabric, while relatively low signals for other peaks were detected due to the F-DLC coating over the nanostructured fabrics (Fig. 2). Therefore, we can conclude that the F-DLC was coated on the superhydrophobic silk fabric surfaces with the peaks of C1s and F1s.[31]

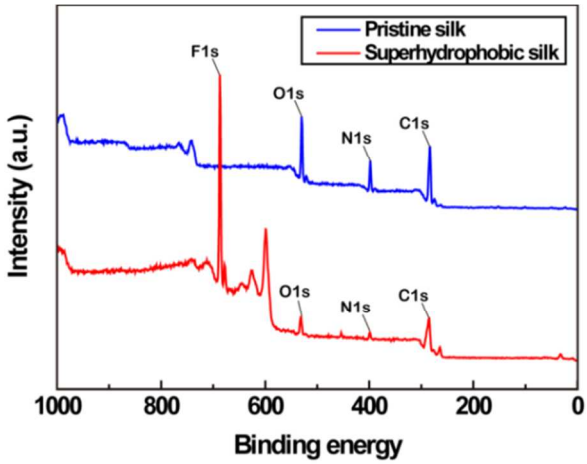

Fig. 2 XPS spectra in survey scans for the pristine (blue line) and the superhydrophobic silk fabric (oxygen ion beam etching for 10 min and F-DLC coating for 30 sec, red line).

Static contact angle and shedding angle

Fig. 3a shows the hierarchical structures having nanostructures on the silk woven fabric, on which the static contact angle and the shedding angle of water droplets were measured on various silk fabric surfaces. After the formation of nanostructures on silk fabrics by the oxygen ion beam irradiation and subsequent deposition of the thin film of low-surface-energy material, the hydrophobicity was observed to significantly increase from near zero for the pure silk fabric to 170º for the nanostructured silk fabric, as shown in Fig. 3b. Note that the pristine silk fabric itself has a hierarchical roughness in two different scales: the fiber itself of 19 μm scale and the fiber bundle on the 2.57 × 1.86 mm/inch scale. In addition, the oxygen ion beam irradiation fabricated a nanoscale roughness on each fiber surface, with nanostructures in the range of 10-50 nm in width and from 10-500 nm in height. Overall, due to at least three different scales in roughness (Fig. 3a), the nanostructured silk fabric easily became superhydrophobic with the addition of the low-surface-energy coating measuring approximately 22 nm in thickness. The pristine silk fabric surface has the static contact angle of near zero, as shown in Fig. 3b, which indicates its fully water absorbing nature due to the hydrophilic characteristic of the protein forming the silk fibers. After the deposition of the low-surface-energy material, the static contact angle rapidly increased with the exposure duration of oxygen ion beam irradiation. The surface became superhydrophobic above 5 min of the oxygen ion beam exposure. Furthermore, the shedding angle was dramatically reduced from 85º, which is the maximum available measurement for shedding angle, to below 10º after 2 min of the oxygen ion beam exposure. As the static contact angle increased to 170º, the shedding angle greatly decreased to nearly zero for the superhydrophobic surface with 10 min etching, as shown in Fig. 3b. Therefore, these results implied that the ion beam treatment for rendering nanostructure on the silk fabric can create a super-water-repellent surface.

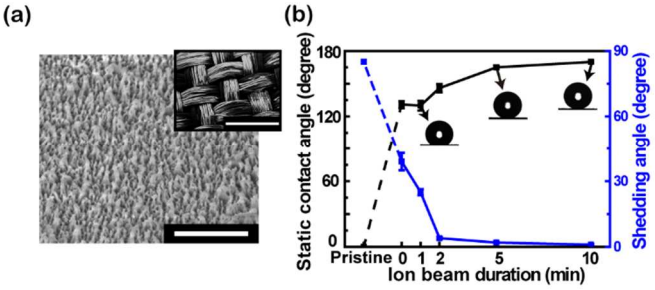

Fig. 3 (a) SEM images of nanostructures formed on a silk fabric exposed by ion beam treatment. The inserted image in (a) shows microscale woven structures of the silk fabric. The scale bars are 1 μm and 400 μm. (b) Static contact angle (black line) and shedding angle (blue line) of a water droplet measured after the 30 sec of hydrophobic coating with various ion beam durations.

Asymmetric wettability and water-drop impact behavior

We explored the water droplet behavior of the silk fabric exhibiting the asymmetric wetting condition of the superhydrophobic silk surface (up-side of the silk fabric) and the pristine silk surface (down-side). One of advantages of the dry etching method is the ability to perform the superhydrophobic treatment on only one side (or up-side) of the silk fabric, producing the static contact angle of 165°, as shown in Fig. 4. The down-side of the superhydrophobic silk fabric retained its original superhydrophilic and water absorbable nature, showing the absorption of a water droplet within 14 sec. It is well-known that garments made of silk fabrics having single-side superhydrophobicity are expected to exhibit breathable and comfortable properties as well as self-cleaning performance.[23] Detailed analysis regarding the silk properties was performed in terms of luster and color of silk fabric before and after the ion beam irradiation.

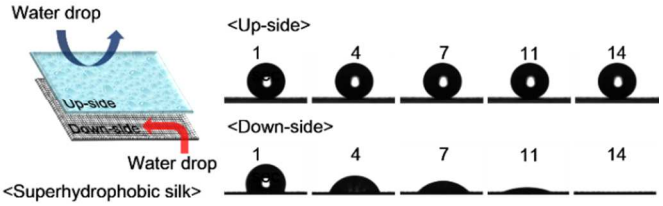

Fig. 4 Absorption behavior of the water droplet on the up-side (nanostructured, superhydrophobic surface) and down-side (pristine surface) of the silk fabric lapsed from 1 to 14 sec.

We also examined the durability of the superhydrophobic fabric with asymmetric wettability by immersing it underwater (Fig. 5a). It was found that after immersing the fabric underwater, the superhydrophobic surface showed with high water contact angle of more than 160° (Fig. 5b), while the opposite hydrophilic surface remained hydrophilic, but the water contact angle was about 15°. Note that the hydrophilic side of the fabric with asymmetric wetting did not absorb water immediately due to the saturation of water into the silk fabric underwater immersing.

Water droplets impacting experiment was performed to simulate the water resistance of a raindrop on the silk fabric with and without the superhydrophobic treatment.

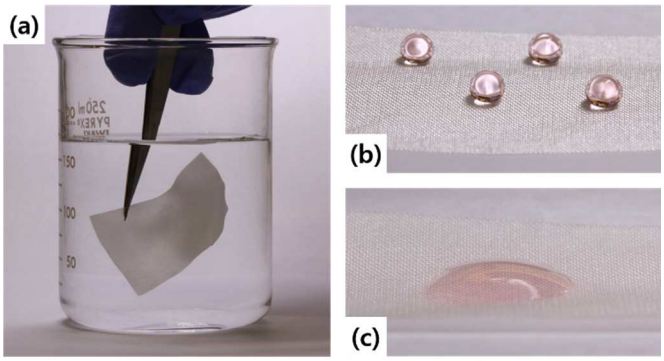

Fig. 5 (a) Optical images of the silk fabric with asymmetric wetting immersed in DI water. (b) The ion beam treated surface (b) and untreated surface (c) of the same fabric maintained superhydrophobicity and hydrophilicity, respectively.

Representative snapshot images of water droplets falling on the pristine and the superhydrophobic silk fabric surfaces are sequentially presented in Fig. 6. A water droplet was immediately absorbed on the pristine silk surface, due to the hydrophilic nature of silk fibers, as shown in Fig. 6a. In contrast, as shown in Fig. 6b, a water droplet bounced on the superhydrophobic silk fabric surface, leaving no residue of water, indicating the high durability in water repellency. This result is induced by the hierarchical structures and lower surface energy of the superhydrophobic fabric (see Fig. 3b). Therefore, it can be considered that clothes produced by the superhydrophobic silk are more resistant to water impact than pristine silk fabric clothes. The static contact angle was not changed even after stretching (upto 40% of strain rate) and bending (upto 180° of bending angle) (Figs. S1 and S2). It is expected that the nanostructures formed on the fiber surface may not be significantly damaged under the macroscopic deformation such as stretching and bending.

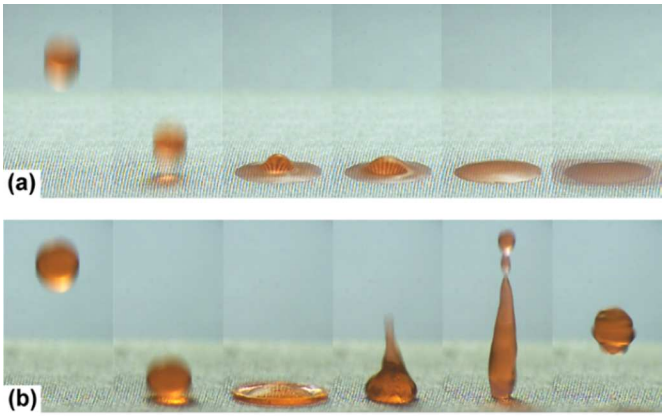

Fig. 6 Bouncing behavior of water droplets on the (a) pristine and (b) superhydrophobic silk fabric.

Measurements of the luster and color values

The luster and color change of samples before and after the ion beam treatment were quantified. Because the luster is a major trait of silk, we investigated the change of luster after the superhydrophobic treatment. The main factors changing luster property were considered to be the nanostructures induced by the oxygen ion beam etching as well as F-DLC coating.

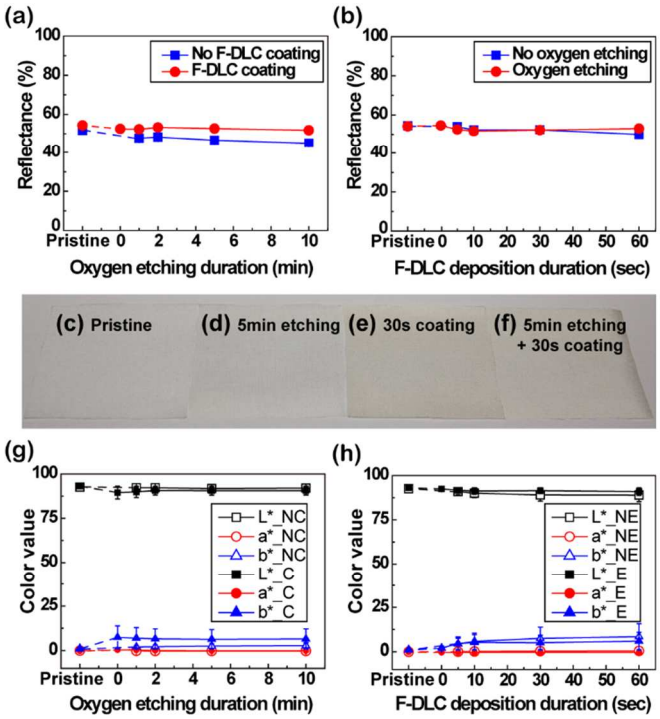

Fig. 7 (a,b) Plots of the average values of luster at every angle of the silk fabrics: (a) various etching duration from 0 to 10 min on the silk fabrics with and without the F-DLC coating for 30 sec. (b) various F-DLC coating duration from 0 to 60 sec on the silk fabrics with and without the oxygen ion beam etching. The oxygen ion beam treatment was performed for 5 min. (c~f) Optical images considering the color change of various silk fabrics. (g,h) Plots of the color changing of the silk surfaces: (g) various etching duration from 0 to 10 min with and without the F-DLC coating for 30 sec and (h) various coating duration from 0 to 60 sec with and without the oxygen etching for 5 min. (L*: darkness index, a*: redness index, b*: yellowing index; NC: no coating, C: coating for 30 sec, NE: no etching, E: etching for 5 min).

First, to examine the effect of nanostructuring by the ion beam etching on luster, the silk fabrics after the exposure duration of oxygen ion beam from 0 (or pristine) to 10 min were examined, as shown in Fig. 7a. With the increase of the ion beam exposure duration, the maximum value for luster decreased before and after the F-DLC coating, reductions of only 7% and 2%, respectively. Note that in comparison to the luster for the etched silk fabrics without the F-DLC coating, the etched silk fabrics after the F-DLC coating increase the luster property. This may be caused by the reduction of nanoscale roughness on the etched silk fabric by the coating with F-DLC film, which results in the relative increase in the reflectance compared to the etched silk fabric surface without the F-DLC deposition. Second, the effect of F-DLC coating on luster was explored by varying the F-DLC deposition duration. The deposition duration of F-DLC at the fixed etching duration of 5 min was varied from 0 to 60 sec, which corresponds to the deposition of no coating to the deposition of 35 nm in the film thickness. With the increase of the deposition duration, the luster was measured to decrease only by 4%, as shown in Fig. 7b. Therefore, compared to the pristine silk fabric, the luster values measured on the superhydrophobic silk fabrics exhibited no difference for the etching duration of less than 10 min and for the deposition of F-DLC of less than 60 sec. Based on these results, it can be concluded that the superhydrophobic treatment on the silk fabric would not alter the luster indices considerably.

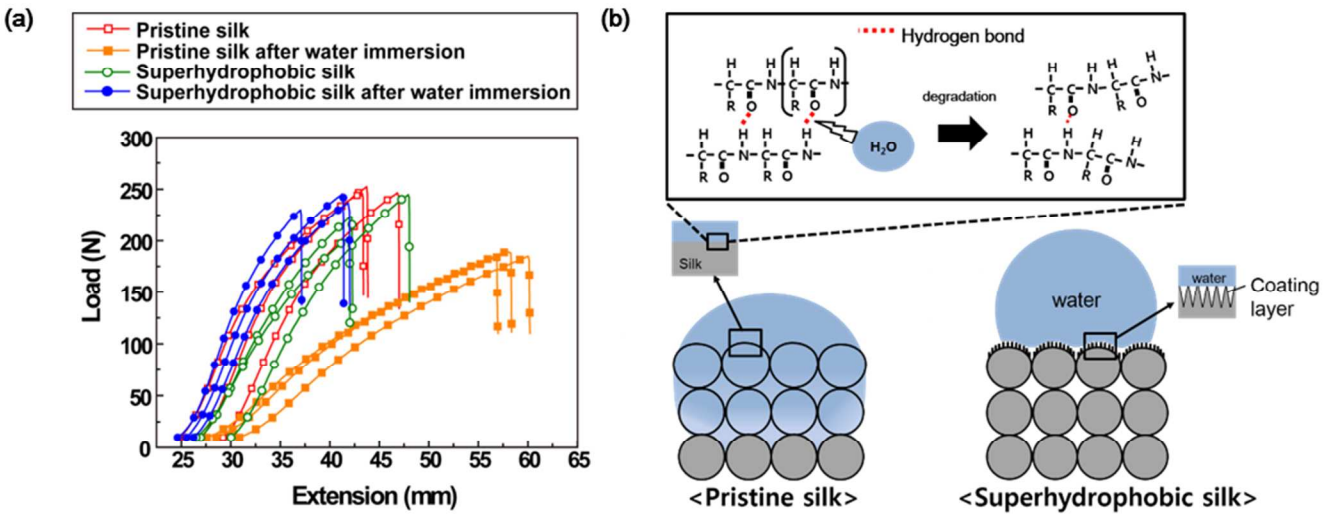

Fig. 8 (a) Load-extension curves of the various silk fabrics with and without water immersion. (b) Illustration of the side view of the silk fabrics with the silk fabrics after water immersion: (left) pristine silk fabric, (right) superhydrophobic silk fabric.

Fig. 7c-f indicates that the color is affected by the F-DLC deposition. The F-DLC coated silk fabric surfaces became relatively darker and yellower than the pristine and ion beam-etched silk surface. The color values of the silk fabrics were investigated by verifying the alteration before and after the oxygen ion beam irradiation and F-DLC deposition (Fig. 7g and h). With only the oxygen ion beam irradiation from 0 to 10 min, the values of L* (darkness index) and b* (yellowing index) on the silk surfaces were found not to change (Fig. 7g). Therefore, within the ion beam irradiation condition chosen in this work, the color changing values remained unchanged. In the case of the silk fabric surfaces with the oxygen ion beam irradiation from 0 to 10 min and subsequent deposition of F-DLC film for 30 sec, the change for L* the b* was slightly increase. For the silk fabric only deposited with the F-DLC deposition, the b*, significantly increased from 1.17 to 8.46 and the L* was reduced with respect to the F-DLC coating duration in various duration (Fig. 7h). Regardless of treating the ion beam etching, the color of silk fabric with the F-DLC coating was changed to dark and yellow. As shown in Fig. 2, after F-DLC coating, the silk fabric surface was covered by an F-incorporated amorphous carbon layer, which exhibits the interference color in yellow, depending on the thickness coated on the surface.[28] Therefore, the covered carbon layer may interfere with the natural color of silk by making it yellower and darker.

Mechanical change before and after pouring water on fabric surfaces

Natural silk has the characteristic of the decrease in the breaking load for the increasing extension due to water wetting. Thus, we measured the dry and wet breaking load of the silk fabrics by performing the mechanical property measurements before and after the water immersion, respectively. As shown in Fig. 8a, the wet breaking load of the pristine silk decreased to 184 N from the value of 247 N for the dry breaking load. However, the wet breaking load of the superhydrophobic silk fabric was almost same as the dry breaking load. In comparison to the pristine silk fabric with the water immersion, the reduction in mechanical property in the superhydrophobic fabric was much smaller. The result can be understood by the fact that, due to the non-wetting condition of the Cassie-Baxter state with low pressure[32] on the superhydrophobic silk surface, the hierarchical structure holds air between the nanostructures, which enables water droplets not to be absorbed through the silk fabric, as illustrated in Fig. 8b (right). However, the pristine silk fabric became weak in the breaking load because the water deposited onto the surface was fully absorbed through the silk fabric and could break the hydrogen bonds in the amorphous region of silk fibers, as illustrated in Fig. 8b (left).[3] Overall, the superhydrophobic silk fabrics induced by the ion beam treatment can enable silk to sustain its mechanical properties in dry or wet conditions.

4. Conclusions

In this study, we fabricated the superhydrophobic silk fabric with 170° of the static contact angle and less than 5° of the shedding angle, which has the high-aspect-ratio nanostructures formed by the selective etching mechanism with the oxygen ion beam irradiation. Because the our two-step manufacturing process, i.e., nanostructuring and subsequent deposition of low-energy materials, can create superhydrophobicity on the one-side of silk fabric, while the other side of the silk fabric remains intact as hydrophilic and water-absorbing, the our method can modify silk fabric to exhibit extremely asymmetric wettability. Such asymmetric wettability improves the moisture transmittance through the fabric or enhances the unidirectional water flow from the skin to the outer surface. After the superhydrophobic treatment, the unique properties of silk such as the luster and color were not changed significantly. In addition, the wet breaking load of the superhydrophobic silk fabrics was measured as not reduced and, rather, as similar to the dry breaking load, due to its non-wetting superhydrophobic nature. Thus, it is expected that the production of superhydrophobic silk fabric without the loss of the unique silk properties would be widely applicable as breathable self-cleaning clothing textiles, such as neckties, blouses and dresses.

Acknowledgements

This work was partially supported from the Global Excellent Technology Innovation R&D Program by the Ministry of Knowledge Economy (MKE), a project No. 10040003 funded by the MKE, and this research was supported by the SRC/ERC

program of MOST/KOSEF (R11-2005-065) and National Research Foundation of Korea (NRF) Grant funded by the Korean Government (2011-0014765).

Notes and references

[a] Department of Clothing and Textiles, Seoul National University, Seoul, 151-742, Republic of Korea. E-mail: junghee@snu.ac.kr

[b] Institute of Multidisciplinary Convergence of Matter, Korea Institute of Science and Technology, Seoul, 136-791, Republic of Korea. E-mail: mwmoon@kist.re.kr

1 K. Mondal, K. Trivedy and S. Nirmal Kumar, *Caspian Journal of Environmental Sciences*, 2007, **5**, 63-76.
2 M. N. Padamwar and A. P. Pawar, *Jounal of Scientific & Industrial Research*, 2004, **63**, 323-329.
3 J. Pe´rez-Rigueiroa, C. Vineyb, J. Llorcaa and M. Elicesa, *Polymer*, 2000, **41**, 8433–8439.
4 J. Caldwell, R. Lunn and A. Ruder, *IARC Monographs*, 1995, **63**, 145-158.
5 S. Li, T. Xing, Z. Li and G. Chen, *Applied Surface Science*, 2013, **268**, 92-97.
6 X. M. Li, D. Reinhoudt and M. Crego-Calama, *Chemical Society reviews*, 2007, **36**, 1350-1368.
7 W. Lee, M.-K. Jin, W.-C. Y. Yoo and J.-K. Lee, *Langmuir : the ACS journal of surfaces and colloids*, 2004, **20**, 7665-7669.
8 J. Li, J. Fu, Y. Cong, Y. Wu, L. Xue and Y. Han, *Applied Surface Science*, 2006, **252**, 2229-2234.
9 H. Perry, A. Gopinath, D. L. Kaplan, L. Dal Negro and F. G. Omenetto, *Advanced Materials*, 2008, **20**, 3070-3072.
10 S. Kim, B. Marelli, M. A. Brenckle, A. N. Mitropoulos, E. S. Gil, K. Tsioris, H. Tao, D. L. Kaplan and F. G. Omenetto, *Nature nanotechnology*, 2014, **9**, 306-310.
11 B. Shin, K.-R. Lee, M.-W. Moon and H.-Y. Kim, *Soft Matter*, 2012, **8**, 1817.
12 N. Zhao, F. Shi, Z. Wang and X. Zhang, *Langmuir : the ACS journal of surfaces and colloids*, 2005, **21**, 4713-4716.
13 J. T. Han, D. H. Lee, C. Y. Ryu and K. Cho, *J. AM. CHEM. SOC.*, 2004, **126**, 4796-4797.
14 A. Nakajima, C. Saiki, K. Hashimoto and T. Watanabe, *JOURNAL OF MATERIALS SCIENCE LETTERS*, 2001, **20**, 1975 – 1977.
15 L. Jiang, Y. Zhao and J. Zhai, *Angew. Chem. Int. Ed.*, 2004, **43**, 4338-4341.
16 M. Ma, Y. Mao, M. Gupta, K. K. Gleason and G. C. Rutledge, *Macromolecules*, 2005, **38**, 9742-9748.
17 S. K. Hodak, T. Supasai, B. Paosawatyanyong, K. Kamlangkla and V. Pavarajarn, *Applied Surface Science*, 2008, **254**, 4744-4749.
18 P. Chaivan, N. Pasaja, D. Boonyawan, P. Suanpoot and T. Vilaithong, *Surface and Coatings Technology*, 2005, **193**, 356-360.
19 S. Li and D. Jinjin, *Applied Surface Science*, 2007, **253**, 5051-5055.
20 K. Kamlangkla, S. K. Hodak and J. Levalois-Grützmacher, *Surface and Coatings Technology*, 2011, **205**, 3755-3762.
21 D. Gogoi, A. J. Choudhury, J. Chutia, A. R. Pal, N. N. Dass, D. Devi and D. S. Patil, *Applied Surface Science*, 2011, **258**, 126-135.
22 D. Gogoi, J. Chutia, A. J. Choudhury, A. R. Pal, N. N. Dass and D. S. Patil, *Plasma Chemistry and Plasma Processing*, 2012, **32**, 1293-1306.
23 Y. Liu, J. H. Xin and C. H. Choi, *Langmuir : the ACS journal of surfaces and colloids*, 2012, **28**, 17426-17434.
24 Y. Kong, Y. Liu and J. H. Xin, *Journal of Materials Chemistry*, 2011, **21**, 17978.
25 H. S. Lim, S. H. Park, S. H. Koo, Y. J. Kwark, E. L. Thomas, Y. Jeong and J. H. Cho, *Langmuir : the ACS journal of surfaces and colloids*, 2010, **26**, 19159-19162.
26 X. J. Su, Q. Zhao, S. Wang and A. Bendavid, *Surface and Coatings Technology*, 2010, **204**, 2454-2458.
27 J. Zimmermann, S. Seeger and F. A. Reifler, *Textile Research Journal*, 2009, **79**, 1565-1570.
28 A. Shirakura, M. Nakaya, Y. Koga, H. Kodama, T. Hasebe and T. Suzuki, *Thin Solid Films*, 2006, **494**, 84-91.
29 M. Isabel Minguez-Mosquer, L. Rejano-Navarro, B. Gandul-Rojas, A. H. Sanchez-Gomez and J. Garrido-Fernandez, *JAOCS*, 1991, **68**.
30 E. K. Her, T. J. Ko, B. Shin, H. Roh, W. Dai, W. K. Seong, H. Y. Kim, K. R. Lee, K. H. Oh and M. W. Moon, *Plasma Processes and Polymers*, 2013, **10**, 481-488.
31 T. Saito, T. Hasebe, S. Yohena, Y. Matsuoka, A. Kamijo, K. Takahashi and T. Suzuki, *Diamond and Related Materials*, 2005, **14**, 1116-1119.
32 C. Luo, M. Xiang, X. Liu and H. Wang, *Microfluidics and Nanofluidics*, 2010, **10**, 831-842.